Study of a Hybrid Pneumatic-Combustion Engine (HPCE) under steady state and transient conditions for transport application

Yidong Fang [a,b], Yiji Lu [a,c,*], Xiaoli Yu [a,c], Lin Su [b], Zhipeng Fan [a], Rui Huang [a], Anthony Paul Roskilly [a,c]

[a] *Department of Energy Engineering, Zhejiang University, Hangzhou 310027, China*

[b] *School of Energy and Power Engineering, University of Shanghai for Science and Technology, Shanghai 200093, China*

[c] *Sir Joseph Swan Centre for Energy Research, Newcastle University, Newcastle NE1 7RU, United Kingdom*

H I G H L I G H T S

- A hybrid pneumatic-combustion engine using compressed air injection boosting is proposed
- The steady state and transient performance of the HPCE are studied
- HPCE can effectively avoid the turbo-lag effect and improve the performance

Abstract

In this study, a new form of hybrid pneumatic combustion engine based on compressed air injection boosting is proposed. The hybrid pneumatic combustion engine regenerates the wasted energy during engine brake to improve the engine performance achieving better fuel economy. The mathematic model of the hybrid pneumatic combustion engine including a supercharged engine and the compressed air tank has been established. The steady state and transient performance of the engine are analysed. Results show that the air injection boosting system can effectively improve the steady-state performance. Under the speed of 1900 r/min and 100% load, the engine torque and power can be increased from 1039 N•m, 206.9 kW to 1057 N•m, 210 kW by adopting air injection boosting with the injection pressure of 0.5 MPa. Effects of air injection parameters are also studied, showing that better performance can be achieved under higher air tank pressure and larger injection hole diameter. In addition, a transient analysis is completed under the speed of 1100 r/min. The result shows that when air injection boosting is used, the responding time of the engine to an instant load increase can be potentially reduced from 5.5 s to 3.5 s under the injection pressure and duration of 0.5 MPa and 3 s. Meanwhile, the tank pressure has limited influence on

* Corresponding author.
E-mail address: luyiji0620@gmail.com; (Y. Lu)

the transient performance of the engine.

Keywords: Hybrid pneumatic combustion engine, air injection boosting, steady state condition, transient condition, performance study

Nomenclature

p	pressure (Pa)	*Greek symbols*	
T	temperature (K)	φ	crank angle (rad)
V	volume (m^3)	λ	excess air factor
m	mass (kg)	ε	ratio of the crank radius to the length
u	specific internal energy (J/kg)		of connecting-rod
h	specific enthalpy (J/kg)	μ	coefficient of flow
Q	heat (J)	Ψ	flow function
W	work (J)	η	efficiency (%)
r	gas constant ($J \cdot kg^{-1} \cdot K^{-1}$)	ω	angular velocity (rad/s)
c_v	specific heat at constant volume	ρ	density ($kg \cdot m^{-3}$)
	($J \cdot kg^{-1} \cdot K^{-1}$)		
V_d	engine displacement (m^3)	*Subscripts*	
S	effective area of intake and exhaust	c	cylinder
	valve (m^2)	W	cylinder wall
h_x	heat transfer coefficient ($W \cdot m^{-2} \cdot K^{-1}$)	B	injected fuel
A_W	area of cylinder wall (m^2)	in	intake
M	torque ($N \cdot m$)	A	exhaust
J	moment of inertia ($kg \cdot m^2$)	t	turbine
		cp	compressor
Abbreviations		f	friction loss
ICE	Internal Combustion Engine	tk	air tank
HPCE	Hybrid Pneumatic-Combustion		
	Engine		
AIB	Air Injection Boosting		
BSFC	Brake Specific Fuel Consumption		

1 Introduction

In order to potentially solve the problems including environmental pollution and the shortage of fossil fuels, various environmental-friendly automobile technologies have been proposed in the past few decades. In addition to the efforts on the design of combustion chamber [1], fuel or water injection strategy [2-4] and alternative fuel [5, 6], the application of hybrid propulsion system is also one of the potential solutions to improve the overall energy fuel saving and reduce the emissions.

The commonly defined hybrid propulsion system is the combination of a conventional Internal Combustion Engine (ICE) and an auxiliary unit driven from clean energy sources. The most well-known one is the hybrid electric vehicle integrating ICE with an electric propulsion system. Alternatively, hybrid pneumatic engine composed of ICE and a compressed air power unit has also attracted growing interests [7-9]. By applying regenerative braking, the hybrid pneumatic engine can recover the waste energy produced during the working process of ICE and store it in the form of compressed air. The engine can be driven by either fossil fuel or compressed air under different conditions. The key advantage of a hybrid pneumatic engine is that different operation modes can be realised in the same power unit since the reciprocating piston structure of ICE can also be used as a compressed air expander. Compared to the hybrid electric system, the system complexity of hybrid pneumatic engine is much lower.

The hybrid pneumatic system integrating a pneumatic power unit to conventional fossil fuelled engine has been applied in fields like power generation and vehicle transportation. For example, Li et al [10] proposed an integration of pneumatic power system and a diesel engine which could be used for electricity generation in isolated areas. Multiple operation modes were designed on the integrated system, including the conventional combustion mode for diesel engine and air motor mode using direct expansion of compressed air.

System evaluation showed that the fuel consumption of the integrated system was 50% of the single diesel engine power generation unit and 77% of a dual diesel unit. Basbous [11-13] applied the concept of the hybrid pneumatic engine on a wind-diesel power generation system. The hybridization was capable of making a diesel engine operating under two-stroke pneumatic motor mode, two-stroke pneumatic pump mode and four-stroke hybrid mode. Zhang et al [14] studied a distributed generation system based on a diesel engine and compressed air energy storage, and the efficiency and fuel saving effect of the integrated system could reach 6.5% and 14.4%, respectively. Saad's calculation showed that the annual fuel savings can reach 60% for the diesel engine after the application of hybrid pneumatic concept [15].

Hybrid pneumatic engine has also been studied for transport application since it is first proposed by Schechter in 1999 [16, 17]. Dimitrova et al [18, 19] applied hybrid pneumatic concept on a C Segment commercial vehicle with 3 cylinder gasoline engine. The hybrid pneumatic powertrain was simulated under different driving cycles and showed an efficiency improvement of 20-50%. The lowest fuel consumption was also evaluated to reach 51 g CO_2/km. Liu [20] and Dou [21] studied the compression process of a hybrid pneumatic engine under different scenarios. Bravo [22] proposed a concept of a hydraulic-pneumatic system for braking energy recovery in heavy-duty vehicles. The simulation showed that the pneumatic hybridization could recover about 10% of total energy under different conditions. Lee [23-25] studied a cost-effective mild hybrid pneumatic engine concept for buses and commercial vehicles. The simulation showed that the fuel mass consumed during the NEDC cycle was 677 g for a standard vehicle and 631.2 g for a hybrid pneumatic vehicle, indicating a fuel saving effect of 6.8%. Wang et al. [26] conducted the simulation study of a hybrid pneumatic engine under urban driving-cycle, showing that the fuel consumption of a light-duty vehicle equipped with a hybrid pneumatic engine can be reduced by 8%. In addition to those mentioned above, a few numerical studies were also reported on the fuel-saving effect of hybrid pneumatic engine in different

applications [27-35].

However, the pneumatic engine driven by compressed air suffers from its relatively low efficiency, which is normally lower than 35% although various optimizations have been used [36-39]. Hence, new methods for the conversion of compressed air energy should be explored, among which the hybrid pneumatic combustion engine using Air Injection Boosting (AIB) system might be a potential solution. The working principle of air injection boosting is to use onboard compressed air to additionally supercharge the engine, as a supplementary for that provided by the turbocharging system. In this paper, the mathematic model of the hybrid pneumatic combustion engine using compressed air injection boosting system was established. The engine performance was analysed under both steady state and transient conditions. Based on the established model, the steady-state and transient analysis on the hybrid pneumatic engine are presented, and the influence of air injection parameters on the engine performance is also studied. The results obtained from this study can be used as a useful and important reference for academic researchers and industrial engine manufacturer.

2 Methodology

2.1 Description of the hybrid pneumatic combustion engine

Fig. 1 illustrates the schematic diagram of a hybrid pneumatic combustion engine. An air injection boosting system is installed on a 6-cylinder diesel engine. The air tank is used to store the compressed air generated from recovering the engine brake energy as described in the previous work [40]. During the regeneration of engine brake energy, the engine is operated as an air compressor, generating compressed air and pump to the air tank through the pipe shown as the red line in Fig. 1.

When the engine is operating for power generation, the exhaust gas flows through the turbine and drives it to rotate, leading to the start of intake air compression by the compressor. The compressed intake air then flows through the intercooler to be cooled down, and finally enters the cylinder and mixes with the injected

fuel. Under most conditions, the engine efficiency will be increased due to the function of turbocharge system. However, the turbocharger system is confronted with low-efficiency issue under transient conditions. For example, the intake flow rate is gradually increased under instant acceleration condition due to the responding period of turbocharges system, causing the turbo-lag effect. Under these circumstances, the compressed air stored in the air tank can be guided through the injection valve into the cylinder to supercharge the engine, which can improve the intake air flow rate and potentially reduce the turbo-lag effect. By adding a compressed air injection boosting system, relatively higher overall system efficiency can be achieved, leading to a better dynamic and economic performance compared to a conventional engine.

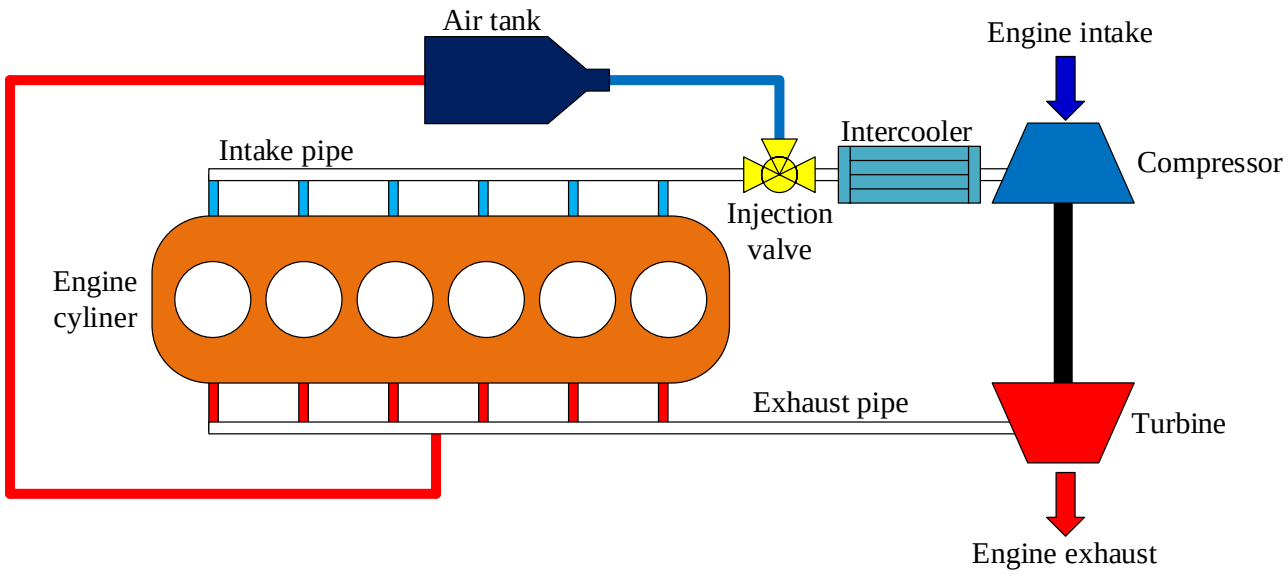

Fig. 1 Schematic of the hybrid pneumatic combustion engine

2.2 Mathematic modelling of the hybrid pneumatic combustion engine

2.2.1 Engine

The working process of the engine is similar to that of a conventional turbocharger engine. Hence, the modelling of the engine can be accomplished based on the theories of an internal combustion engine. Fig. 2 illustrates the control volume of the engine cylinder, where p_c, T_c, V_c, m_c and u_c represent the pressure, temperature, volume, mass and specific internal energy of the in-cylinder gas, respectively; The pressure,

temperature, enthalpy and mass flow rate of the intake and exhaust are represented by p, T, h and dm, with the subscript in indicating the intake and A indicating the exhaust. m_B and Q_B are the mass and combustion heat of the fuel injected into the cylinder, while φ and W respectively indicate the crank angle and work.

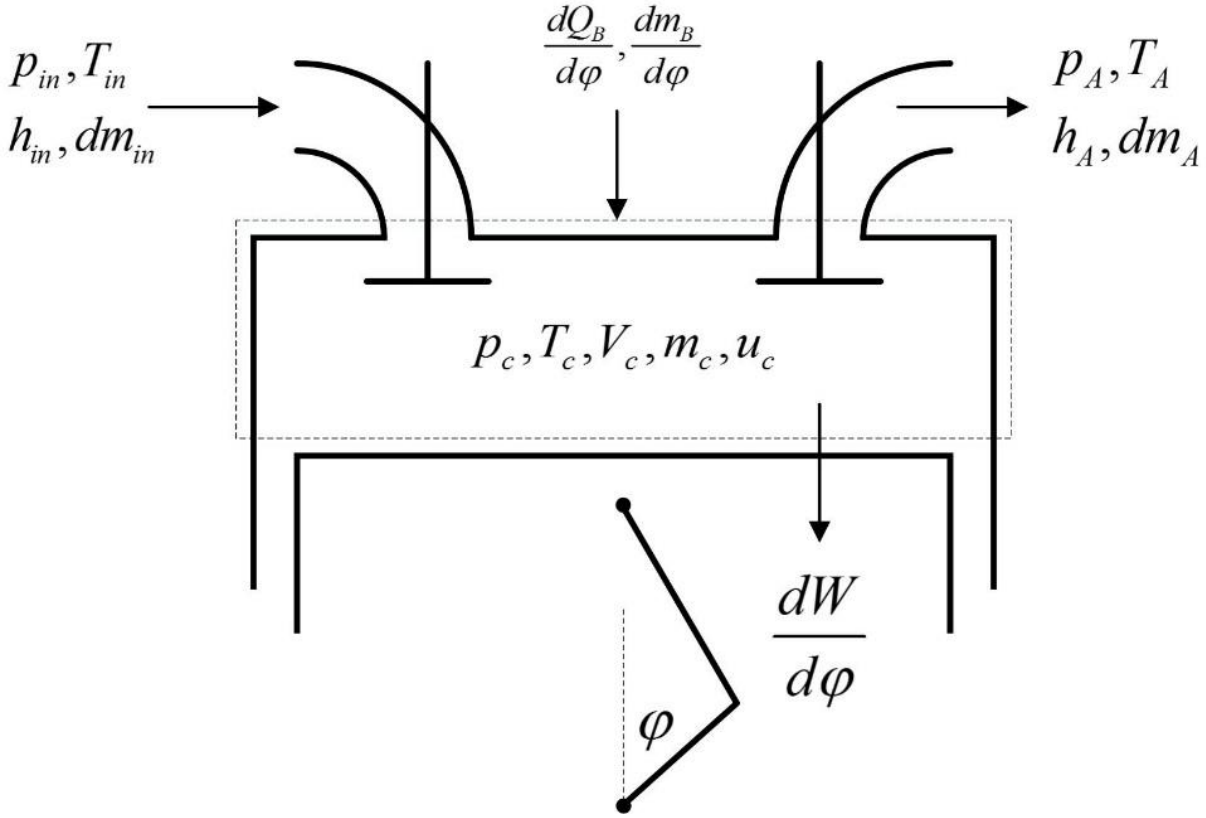

Fig. 2 Schematic of the cylinder control volume

Based on the above assumptions, the in-cylinder temperature can be expressed as

$$\frac{dT_c}{d\varphi} = \frac{1}{mc_v} \cdot \left(\frac{dQ_B}{d\varphi} + \frac{dQ_W}{d\varphi} - p_c \frac{dV_c}{d\varphi} + h_{in} \frac{dm_{in}}{d\varphi} - h_A \frac{dm_A}{d\varphi} - u_c \frac{dm_c}{d\varphi} - m_c \frac{\partial u_c}{\partial \lambda} \frac{d\lambda}{d\varphi} \right) \tag{1}$$

where c_v is the specific heat of the gas in the cylinder.

The mass conservation of the cylinder control volume and the ideal gas law can be expressed in the following equations.

$$\frac{dm_c}{d\varphi} = \frac{dm_B}{d\varphi} + \frac{dm_{in}}{d\varphi} - \frac{dm_A}{d\varphi} \tag{2}$$

$$p_c V_c = m_c r T_c \tag{3}$$

where r is the gas constant, and it can be obtained r=289 J/(kg·K) for air.

In addition to the above equations, extra equations describing the boundary conditions are required and listed as follows.

The instant cylinder volume is demonstrated in Eq (4)

$$\frac{dV_c}{d\varphi} = \frac{V_d \sin\varphi}{2}\left(1 + \frac{\varepsilon\cos\varphi}{\sqrt{1-\varepsilon^2\sin^2\varphi}}\right) \tag{4}$$

where, V_d is the engine displacement, and ε is the ratio of the crank radius to the length of connecting-rod.

The intake and exhaust mass flow rate is expressed as

$$\frac{dm}{d\varphi} = \mu S\psi\sqrt{2p_1\rho_1} \tag{5}$$

where S is the effective area of intake and exhaust valve, and μ is coefficient of flow; p_1, ρ_1 is the pressure and density of the fluid at the upstream of the valves, respectively. Ψ is the flow function determined by the pressure ratio between the up- and downstream fluid.

The heat due to the fuel combustion is expressed by Weibe function according to Ref [41], while the heat transfer between the gas and cylinder wall is demonstrated as follow.

$$\frac{dQ_W}{d\varphi} = h_x A_W\left(T_W - T_c\right) \tag{6}$$

where A_W is the effective heat transfer area of the cylinder wall, and T_W is the cylinder wall temperature. h_x is the heat transfer coefficient between the gas and cylinder wall, obtained according to Woschni empirical equation. The equations listed above were embedded in the simulation software GT-SUITE, thus completing the modelling of the engine. It should be note that the accurate description of the heat transfer and combustion of diesel engine requires a sufficient understanding on different physical and chemical processes occur during the engine operation, which was unable to be achieved without the studies on processes such as air motion in the cylinder or the fuel spray break-up or penetration. In order to simplify the modelling of the engine, the tuning constants of Woschni equation and Weibe function were set according to the recommended values

provided by GT-SUITE, which covers various conditions including different engine speeds and air fuel ratios.

2.2.2 Turbocharger system

The turbocharger system is composed of the turbine, the compressor and the mechanical connecting shaft, where the powers of the turbine and compressor are expressed as follows.

$$\frac{dW_{cp}}{d\varphi}=\frac{dm_{cp}}{d\varphi}\cdot\frac{1}{\eta_{cp}}\cdot\left[\left(\frac{p_{cp2}}{p_{cp1}}\right)^{\frac{k-1}{k}}-1\right] \tag{7}$$

$$\frac{dW_{t}}{d\varphi}=\frac{dm_{t}}{d\varphi}\cdot\eta_{t}\cdot\left[1-\left(\frac{p_{t2}}{p_{t1}}\right)^{\frac{k-1}{k}}\right] \tag{8}$$

W_{cp} and W_t are the power consumption and output of compressor and turbine, respectively. m and η represent the mass flow rate and efficiency, with the subscript cp and t indicating the compressor and the turbine. p_{cp2} and p_{cp1} are the pressures at the outlet and inlet of the compressor, while p_{t2} and p_{t1} stand for those of the turbine.

Except for the power, the torque balance of the turbocharger system is described by

$$M_t-M_c-M_f=J_t\frac{d\omega_t}{dt} \tag{9}$$

M_t, M_c and M_f represent the torque of the turbine, compressor and friction loss, respectively. J_t is the moment of inertia of turbine, and $d\omega_t/dt$ is the angular acceleration.

2.2.3 Compressed air tank

The modelling of the air tank is similar to that of the engine cylinder since the air tank can also be considered as a control volume, hence the air temperature and pressure in the tank can be expressed as

$$\frac{dT_{tk}}{d\varphi}=\frac{1}{m_{tk}c_v}\cdot\left(\frac{dQ_{tk}}{d\varphi}+h_t\frac{dm_{tk}}{d\varphi}\right) \tag{10}$$

$$p_{tk}V_{tk}=m_{tk}rT_{tk} \tag{11}$$

dQ_{tk} is the heat transfer rate between the air tank and ambient, which can be neglected if the air tank is well

insulated. $dm_{tk}/d\varphi$ is the mass flow rate of the air entering or exiting the air tank and can be derived by assuming an adiabatic flow process of air.

2.3 Experimental validation

A 6-cylinder diesel engine has been used for modelling and experimental validation, and the specification of the engine is listed in Table 1.

Table 1 Engine specification

Item	Unit	Value
Displacement	L	7.1
Bore	mm	108
Stroke	mm	130
Connection rod length	mm	209.7
Compression ratio	-	17.6
Clearance height	mm	0.5
Intake valve timing	-	20°BTDC-25°ABDC
Exhaust valve timing	-	55°BBDC-20°ATDC

The engine was operated under 100% load during the validation experiment, while the speed was varied from 900 r/min to 2300 r/min. The map of the fuel injection and supercharge system of the simulation model is also identical to that of the real engine. The comparison between the experimental and simulation results is illustrated in Fig. 3. It can be seen that when the engine is operated under full load, the error of engine power between the experiment and simulation is below 4%, while the error of engine BSFC is approximately 3%. It should also be noted that the simulation error under part load conditions is expected to be approximately 5% since the different air fuel ratios were considered during the modelling. The engine model can therefore be regarded as reliable and suitable for further numerical analysis.

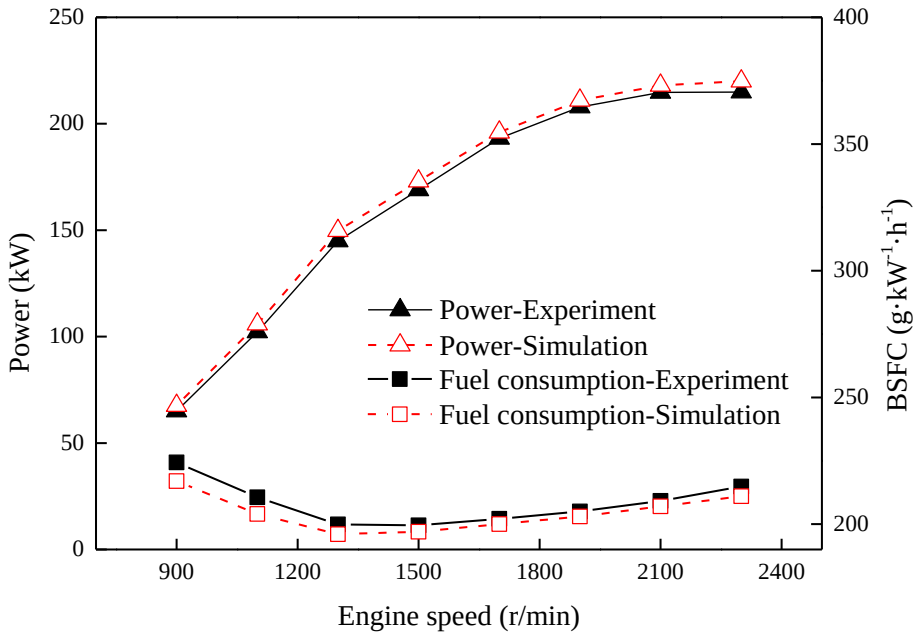

Fig. 3 Comparison between the simulation and experimental results

3 Results and discussion

The engine model was established according to the equations listed above, together with the air injection boosting system, followed by the analysis on the engine performance under different conditions to justify the effects of Air Injection Boosting (AIB) on the performance parameters of the engine. During the analysis, the engine was set to be operated under different speeds ranging from 1000 r/min to 1900 r/min, and the engine load is varied from 20% to 100%. The mass of the fuel injected into the cylinder of the original engine was set identical to that after the application of air injection boosting under the same load and speed. The pressure of the air tank was set to constant to achieve a steady state analysis, while a certain tank volume was set during transient analysis together with initial tank pressure.

3.1 Effects of air injection boosting under steady state conditions

Fig. 4 illustrates the intake mass flow rate of the engine under different conditions. It should be noted that the tank pressure is 0.5 MPa when the air injection boosting is adopted, while the diameter of the injection hole is 5 mm. Results indicate the intake mass flow rate is increased after the air injection boosting is adopted.

The explanation is that the intake flow consists of two streams when the air injection boosting is used, which is a mixture of compressed air from the compressor with lower pressure and the compressed air injected into the intake pipes through the injection valve. Therefore, the total mass flow rate of the intake is larger than that of the original engine without air injection boosting.

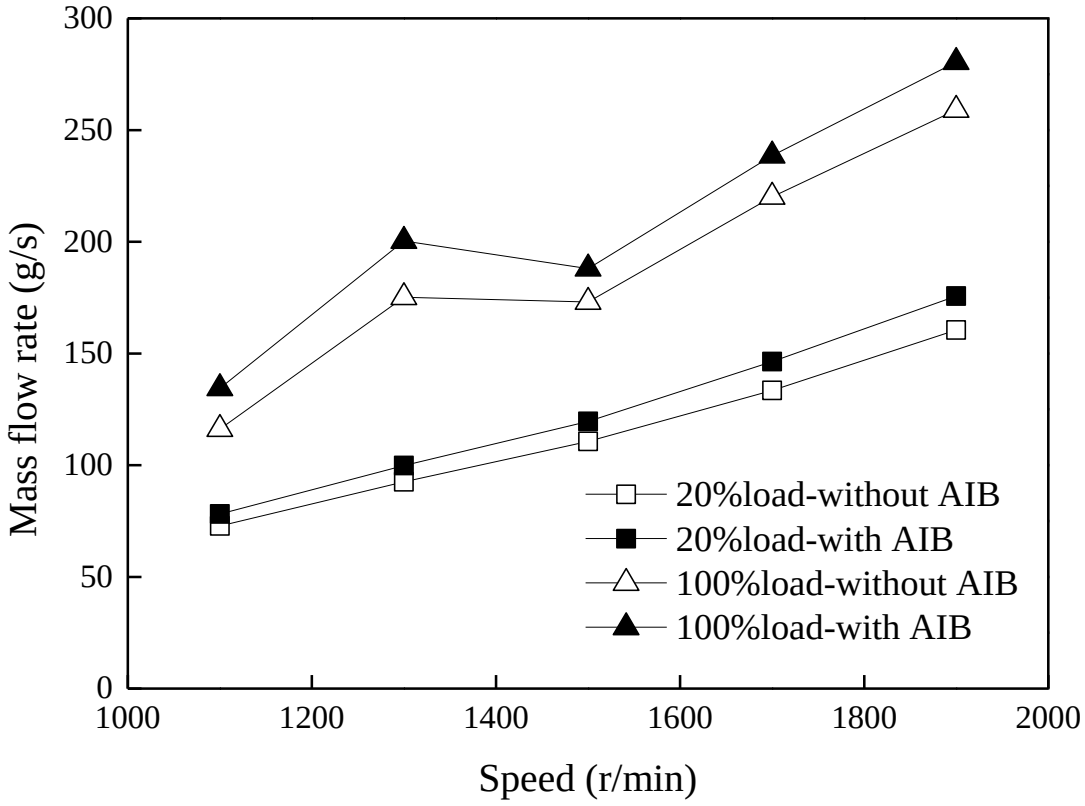

Fig.4 Intake mass flow rates of the engine under different conditions

The effects of air injection boosting (AIB) on the torque and power of the engine are illustrated in Fig. 5, Fig. 6 and Table 2. Results indicate the torque and power of the engine are both increased by adding the air injection boosting system. For example, when the engine is operating without air injection boosting system, the torque and power are 213 N·m and 42.5 kW under the speed of 1900 r/min and 20% load condition. When the air injection boosting is used, the engine torque and power are improved to 215 N·m and 43 kW, respectively. When the load is set to 100%, the engine torque and power are 1039 N·m and 206.9 kW without air injection boosting under the speed of 1900 r/min shown in Fig. 6. After the application of AIB, the torque

and power can be improved to 1057 N·m and 210 kW, respectively. The improvement of the fuel combustion process inside the engine cylinder is the one of the reasons for this improvement. The intake mass flow rate can be increased when the air injection boosting is activated, leading to an increase in the amount of the fresh charge. Consequently, the in-cylinder pressure at the end of the compression stroke is increased, promoting the break-up process of diesel droplets, finally improving the combustion process. As shown in Fig. 7, the peak in-cylinder pressure is raised from 12.5 MPa to 14 MPa with the application of air injection boosting at 1500 r/min and 100% load. Other possible reason is that the pumping process is also improved by adopting the air injection boosting due to a higher intake manifold pressure caused by compressed air injection. As shown in Fig.8, the open cycle efficiency [42] of the engine is also improved by 1%~2% under various speeds and loads, indicating that a more efficient gas exchange process and lower negative pumping work can be achieved by adopting air injection boosting.

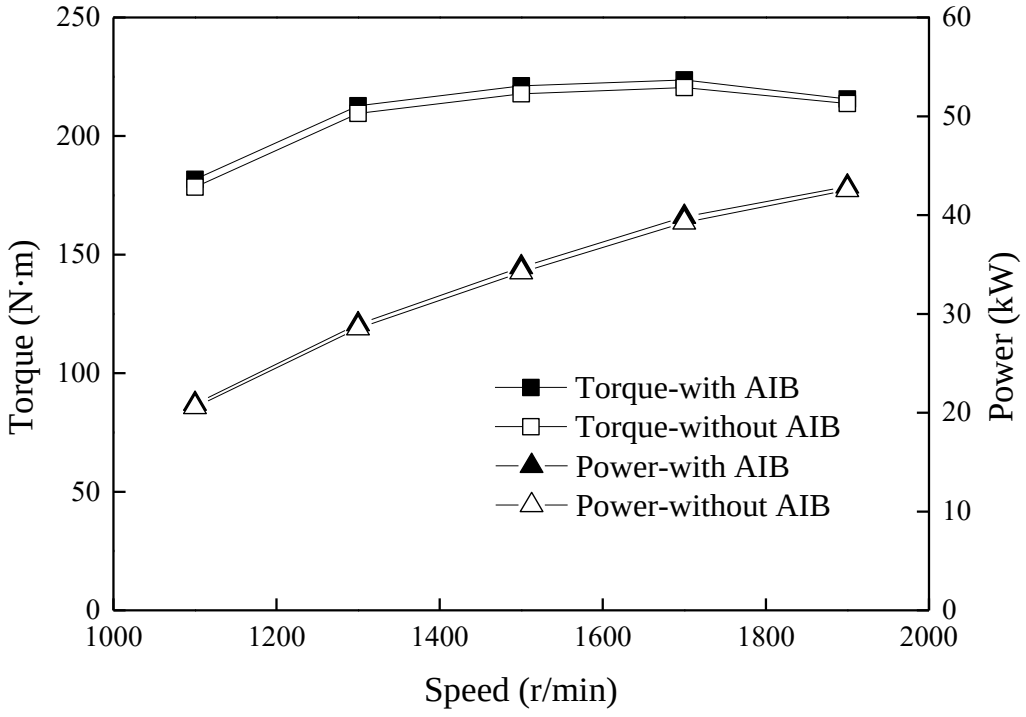

Fig.1 Torque and power of the engine under 20% load

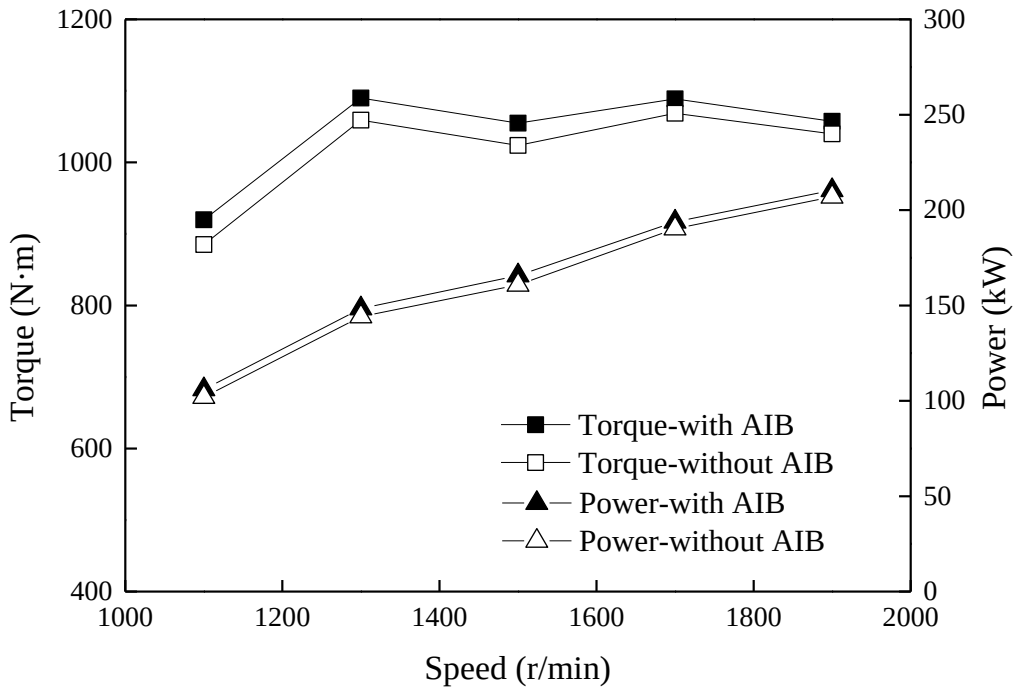

Fig.2 Torque and power of the engine under 100% load

Table 2 Torque and power of the engine under various loads

Load	Speed (r/min)		1100	1300	1500	1700	1900
20%	Torque (N·m)	without AIB	178.5	209.6	217.8	220.4	213.7
		with AIB	**181.7**	**212.8**	**221.2**	**223.7**	**215.6**
100%		without AIB	885.1	1059.0	1023.7	1068.8	1039.8
		with AIB	**919.8**	**1089.9**	**1054.9**	**1088.9**	**1057.5**
20%	Power (kW)	without AIB	20.6	28.5	34.2	39.2	42.5
		with AIB	**20.9**	**29.0**	**34.7**	**39.8**	**42.9**
100%		without AIB	102.0	144.2	160.8	190.3	206.9
		with AIB	**106.0**	**148.4**	**165.7**	**193.9**	**210.4**

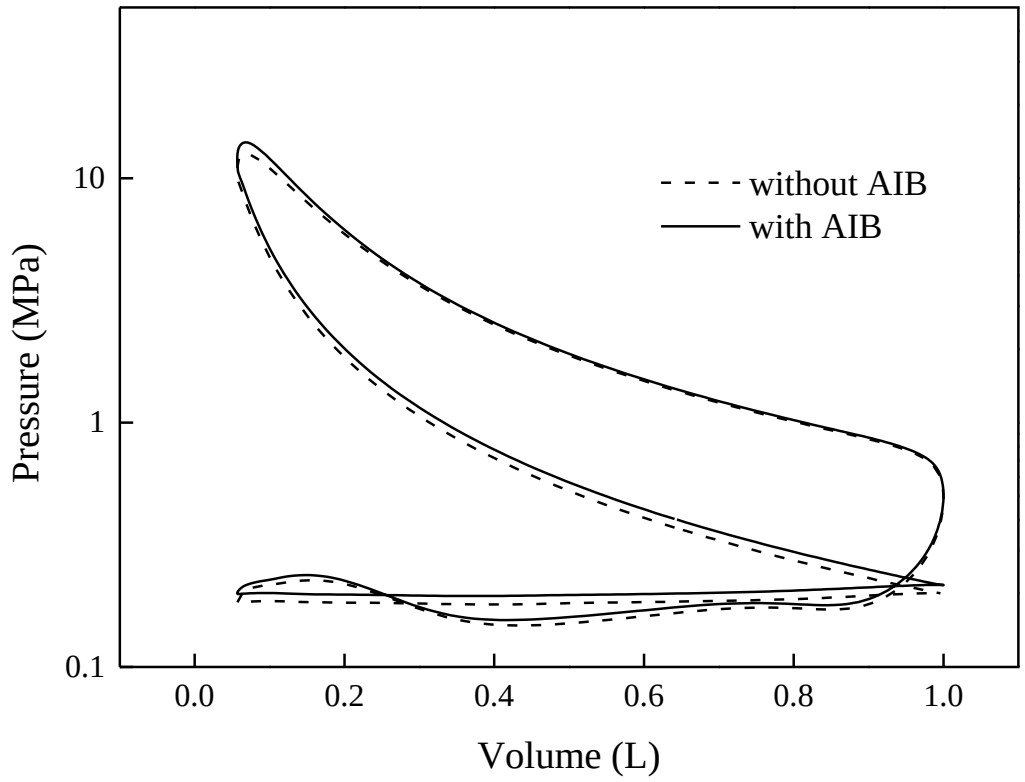

Fig.7 Comparison of in-cylinder pressure of the engine (100% load, 1500 r/min)

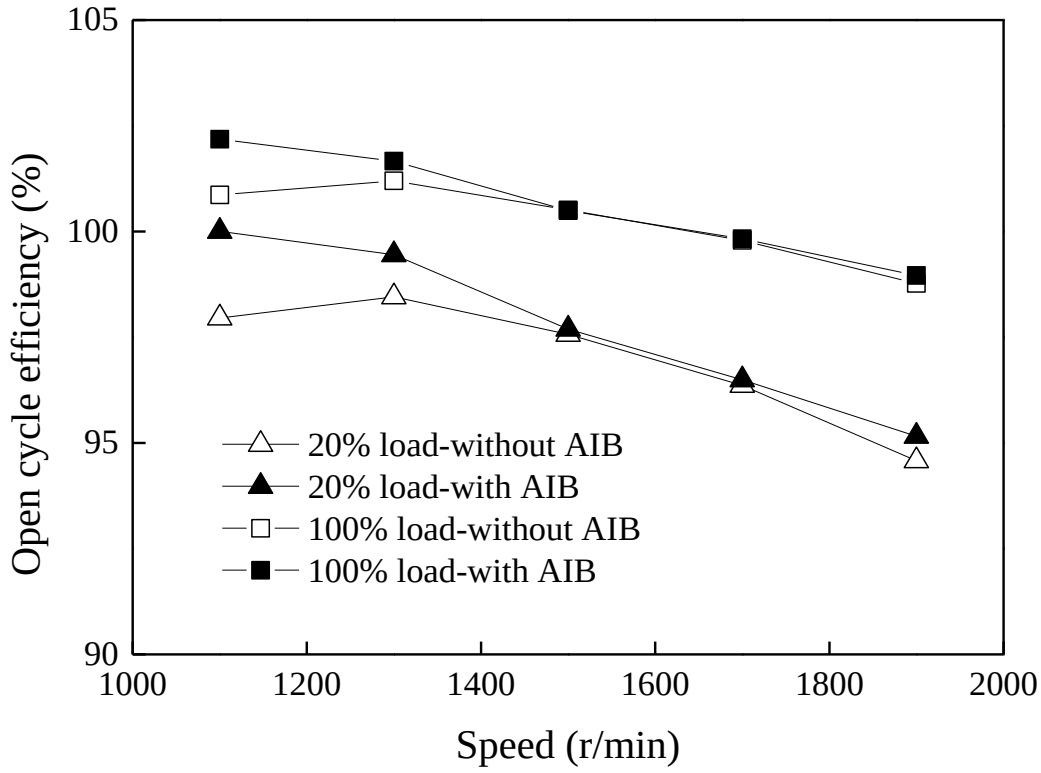

Fig.8 Open cycle efficiency of the engine under different conditions

Fig. 9 shows the comparison of the engine BSFC with or without the application of the air injection

boosting. Similar improvements of the fuel economy can be observed under different engine loads. At 20% load, the lowest BSFC of 245 g/(kW·h) can be achieved at the speed of 1500 r/min, while it is decreased to 241 g/(kW·h) after the application of air injection boosting, indicating an improvement of 1.6% in BSFC. The values are 200 g/(kW·h) and 195 g/(kW·h) when the engine load is raised to 100%, respectively, showing an improvement of 2.5%. The reduction of BSFC can be attributed to the improvement of the engine power, as shown in Fig. 5. Since the mass of the fuel injected remains constant, the increased engine power results in the reduction of BSFC.

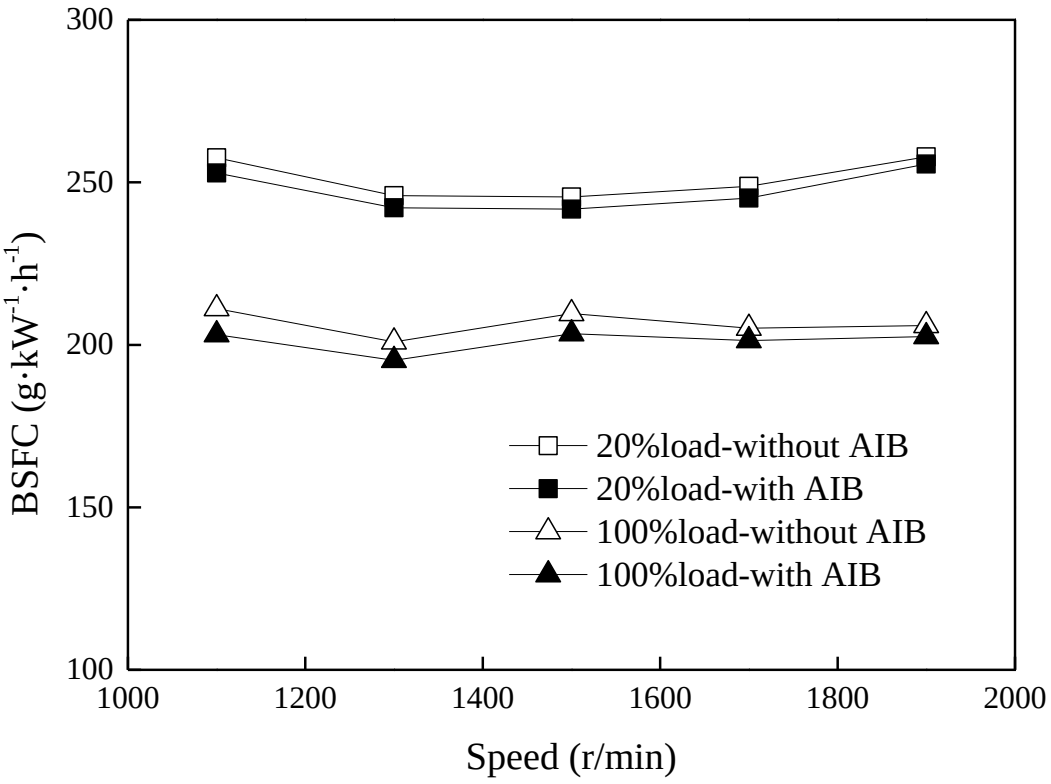

Fig.9 Engine BSFC under different conditions

3.2 Effects of air injection parameters on engine performance

Engine performance is also analysed in this section with different parameters of air injection boosting, including the tank pressure and diameter of the injection hole. During the analysis, the engine speed was set to 1100 r/min during the analysis for the convenience, while the engine load varied from 20% to 100%. Fig. 10

shows the variation of in-cylinder pressure of the engine versus air tank pressures under the speed of 1100 r/min and 100% load. It should be noted that the pressure of the air tank can be changed by the adjustment on the compressed air regenerative braking system in the practical application. As shown in Fig. 10, higher peak in-cylinder pressure of the engine can be achieved under higher air tank pressure. A peak pressure of 13 MPa can be observed when the air tank pressure is 0.3 MPa, while it can be increased to 14.7 MPa if the tank pressure is raised to 0.7 MPa. One of the reasons for the variation of the in-cylinder pressure is the improvement of the fuel combustion process under higher air tank pressure. When the air injection boosting is applied, the amount of fresh charge in the cylinder is increased under higher air tank pressures, leading to more sufficient combustion of the diesel-air mixture. Other possible reason is that the pumping process is also optimized with higher air tank pressure, leading to a more efficient gas exchange process.

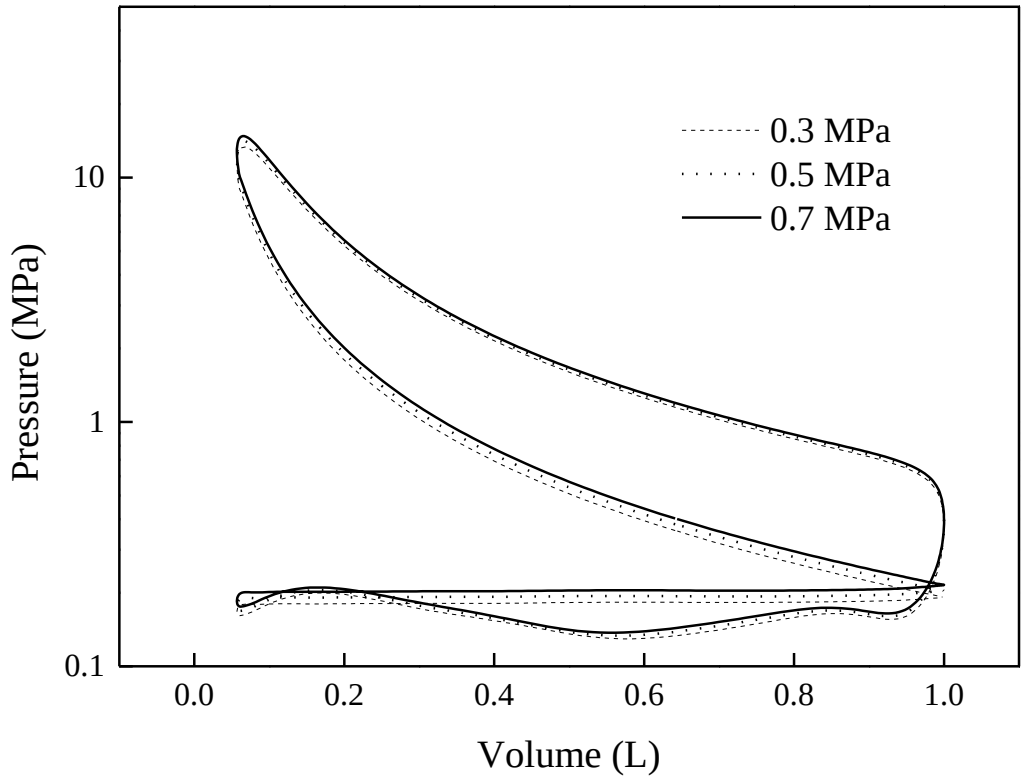

Fig.10 In-cylinder pressure of the engine under different tank pressures

The variations of the power and BSFC of the engine are shown in Fig. 11 and Table 3. It can be

concluded that the increase of air tank pressure can lead to a better performance of the engine in both power and fuel economy. It can also be observed that the difference in power and BSFC become more obvious under high engine loads, indicating that the air injection boosting with higher air tank pressure might be more effective when the engine is operated under high load.

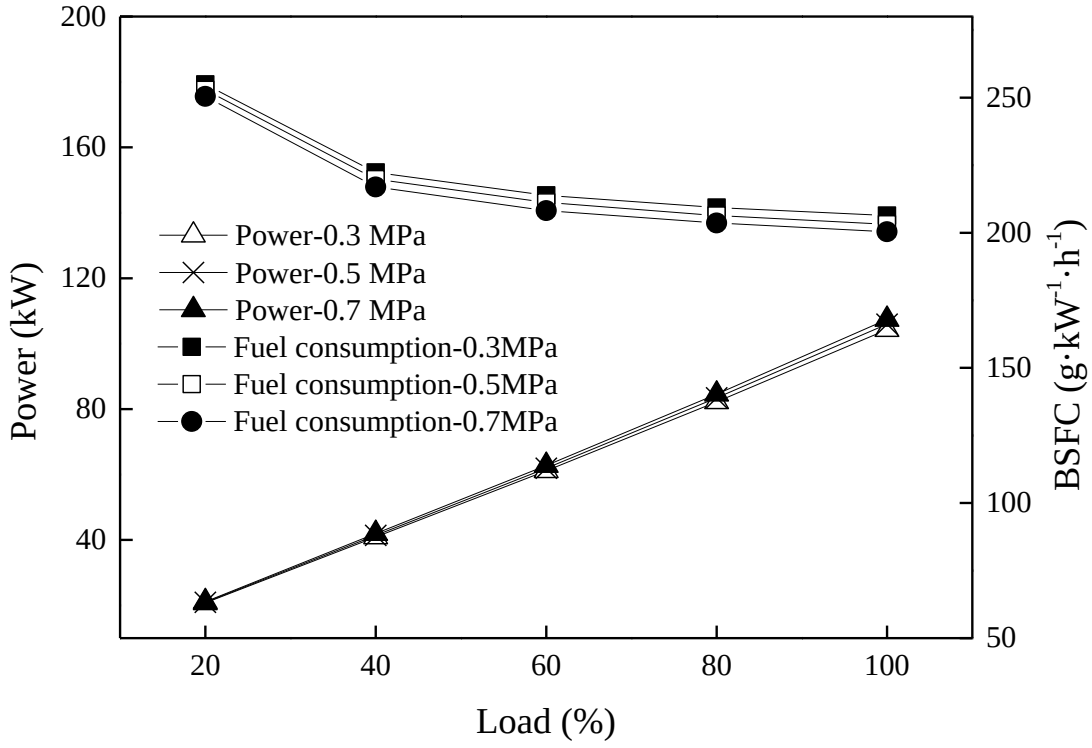

Fig.11 Power and BSFC of the engine under different air tank pressures

Table 3 Power and BSFC under different air tank pressures

Tank Pressure (MPa)	Load (%)	20	40	60	80	100
0.3	Power (kW)	20.8	40.9	61.1	82.3	104.3
	BSFC (g·kW^{-1}·h^{-1})	254.9	222.3	213.8	209.3	206.4
0.5	Power (kW)	20.9	41.4	61.9	83.4	106.0
	BSFC (g·kW^{-1}·h^{-1})	252.9	219.8	211.2	206.4	203.2
0.7	Power (kW)	21.1	42.0	62.8	84.6	107.4
	BSFC (g·kW^{-1}·h^{-1})	250.5	216.9	208.2	203.6	200.4

The effects of the diameter of air injection hole on the engine performance have also been analysed. Note that the diameter of the injection hole refers to the hydraulic diameter, and can be changed by adjusting the

cross-section area of the flow path in the air injection valve. As shown in Fig. 12 and Table 4, the enlargement of the hole diameter can lead to better power and economic performance of the engine. Under 1100 r/min and 100%, an improvement of 5.8% can be achieved on the engine power. Meanwhile, the BSFC is lowered by 5.5% if the diameter of the air injection hole is increased from 3 mm to 7 mm. The improvement of the fuel combustion and pumping process under larger hole diameters are the possible reasons for the variation trend. However, it should be noted that the mass flow rate of the injected air can be inevitably increased when the hole diameter is enlarged, indicating a higher consumption rate of compressed air recovered from the regenerative braking. Therefore, the determination of the size the injection hole should be based on a comprehensive consideration of the performance improvement and the consumption rate of the compressed air during real practice.

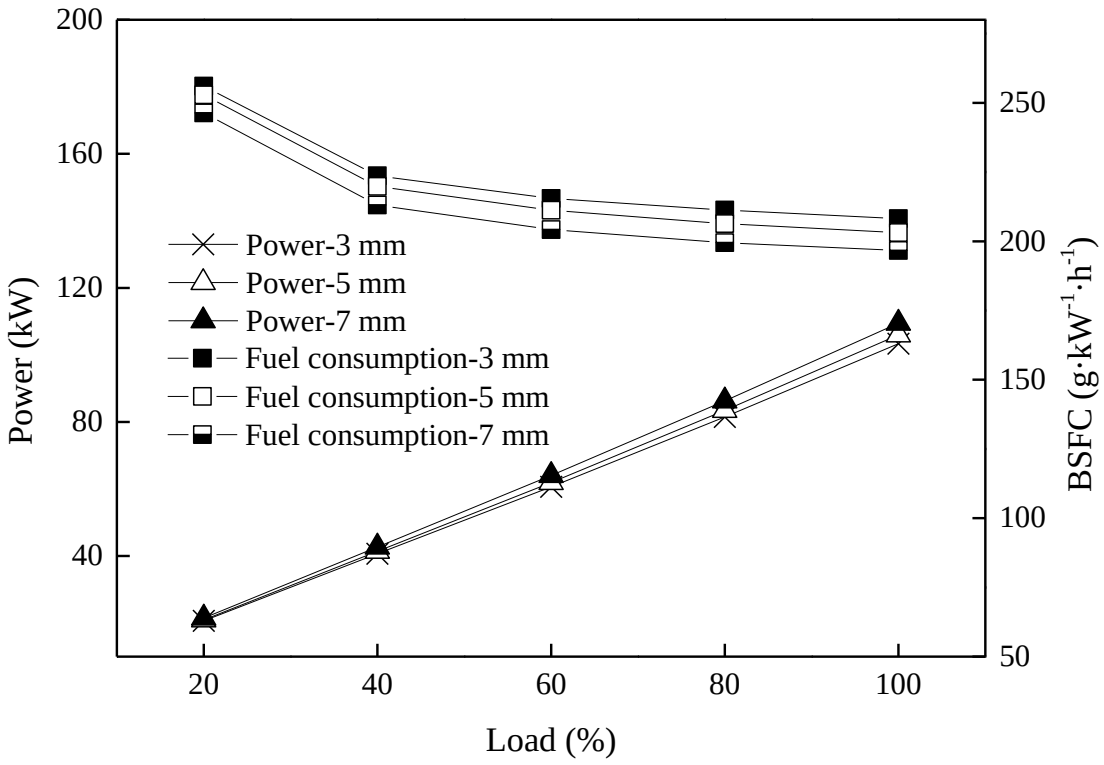

Fig.12 Power and BSFC of the engine under different injection hole diameters

Table 4 Power and BSFC under different injection hole diameters

Tank Pressure (MPa)	Load (%)	20	40	60	80	100

0.3	Power (kW)	20.8	40.9	61.1	82.3	104.3
	BSFC ($g \cdot kW^{-1} \cdot h^{-1}$)	254.9	222.3	213.8	209.3	206.4
0.5	Power (kW)	20.9	41.4	61.9	83.4	106.0
	BSFC ($g \cdot kW^{-1} \cdot h^{-1}$)	252.9	219.8	211.2	206.4	203.2
0.7	Power (kW)	21.1	42.0	62.8	84.6	107.4
	BSFC ($g \cdot kW^{-1} \cdot h^{-1}$)	250.5	216.9	208.2	203.6	200.4

3.3 Analysis under transient conditions

The previous analyses indicate that the performance of the engine can be improved by adopting in-cylinder boosting based on compressed air injection. In addition to the improvement under steady state conditions, an important function of air injection boosting is to overcome the turbo-lag effect of the engine during transient conditions such as acceleration or sudden torque variation. Therefore, the transient performance of the engine equipped with air injection boosting system is analysed and discussed in this section.

As for the transient analysis, the engine specification remains the same as shown in Table 1. In order to simulate a real source of compressed air, an air tank with a volume of 150 L is added to the model. The operation conditions of the engine are set as listed in Table 5. The engine speed remains stable at 1100 r/min during the whole process. The initial engine load is maintained at 20% for 5 s, and then increased to 100% in 0.5 s to simulate an instant load increase. After that, the engine load is maintained at 100% while the speed remains stable at 1100 r/min for 10 s. The compressed air will be injected into the intake port through a hole with the diameter of 5 mm, and the injection is activated at t=5.1 s. The initial pressure of the tank and injection duration are set differently to justify the effects of air injection boosting on the transient performance of the engine during the process.

Table 5 Transient operation conditions of the engine

Time	Engine load	Engine speed
0 ~ 5 s	20%	1100 r/min
5 ~ 5.5 s	linear increase from 20% to 100%	1100 r/min
5.5 ~ 15.5 s	100%	1100 r/min

The torque variation of the engine during the transient process is illustrated in Fig. 13. As shown in the figure, the torque of the engine basically remains stable at about 180 N·m until t=5 s. When the load is increased from 20% to 100%, the torque rises quite fast at the beginning, then gradually stabilises at 875 N·m. The load variation is completed within 0.5 s, however it takes more than 4 s for the torque to reach a stable output, indicating the existence of turbo-lag effect during the transient process. It can also be noted the increase rate of torque is different under different compressed air injection durations. When the injection duration is 0 s, indicating the deactivation of air injection boosting, the torque reaches 875 N·m at t=11 s, about 5.5 s after the completion of the load increase process. However, the time gap is narrowed down to 3.5 s if air injection boosting with an injection duration of 3 s is activated, showing a better transient response of the engine. If the air injection duration is further increased to 4 s, the torque even excesses 875 N·m at t=8 s, then gradually decreases to 875 N·m in about 2 s, as shown in Fig. 13.

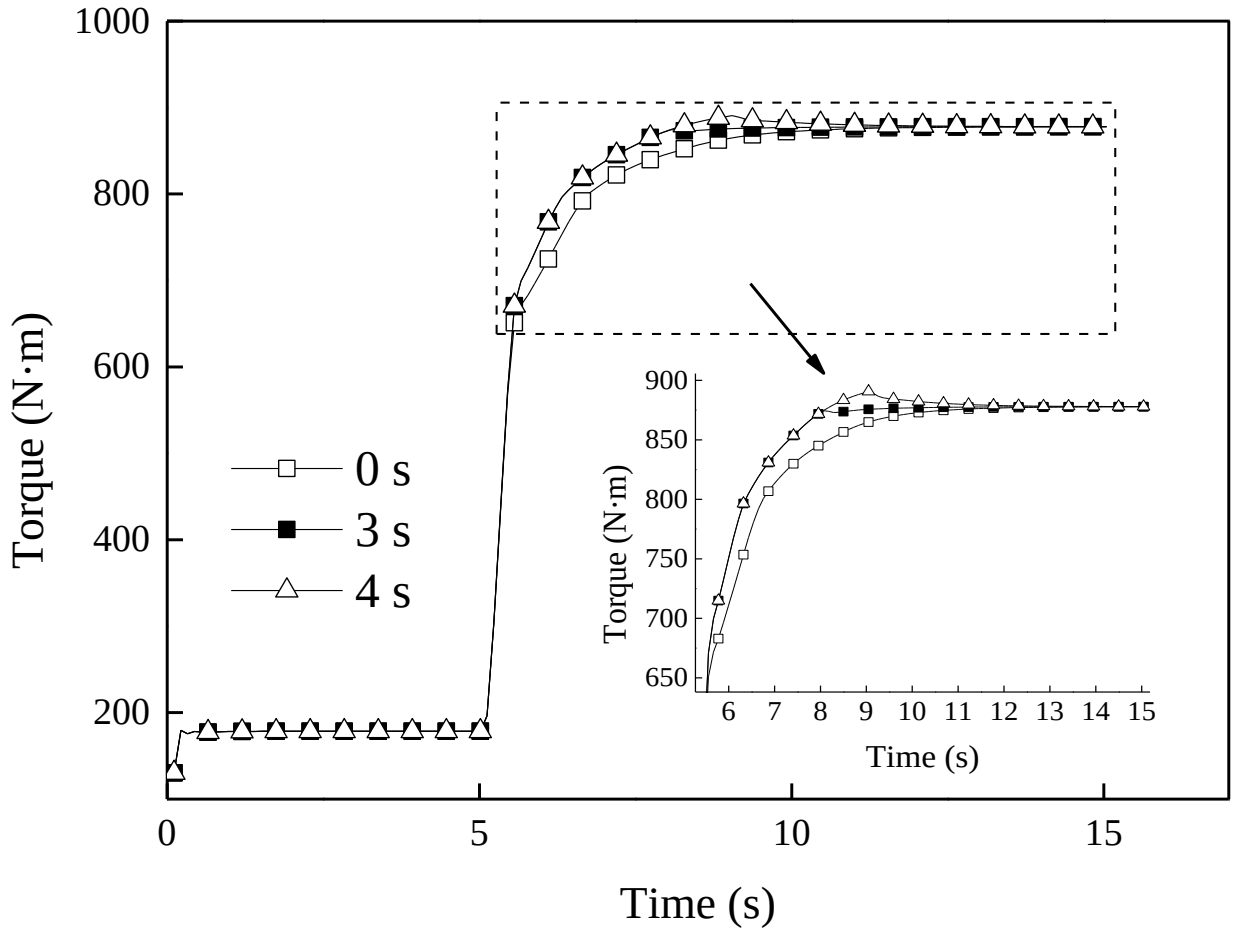

Fig. 13 The torque of the engine under different air injection durations

The difference of the torque variation can be attributed to the increase of intake mass flow rate during the transient process. When confronting an instant load increase, a short period of time is required for the turbocharging system to re-stabilize, leading to the shortage of intake air during the transient process, hence the torque of the engine is unable to increase as quickly as the load. However, the shortage of the intake air can be supplemented by the activation of air injection boosting. As shown in Fig. 14, the increase rate of intake flow mass becomes larger when the air injection boosting is adopted, hence the amount of air entering the cylinders can be raised during the transient load increase process, thus improving the combustion process and reducing the negative pumping work of the engine, eventually achieving a better transient response of the engine.

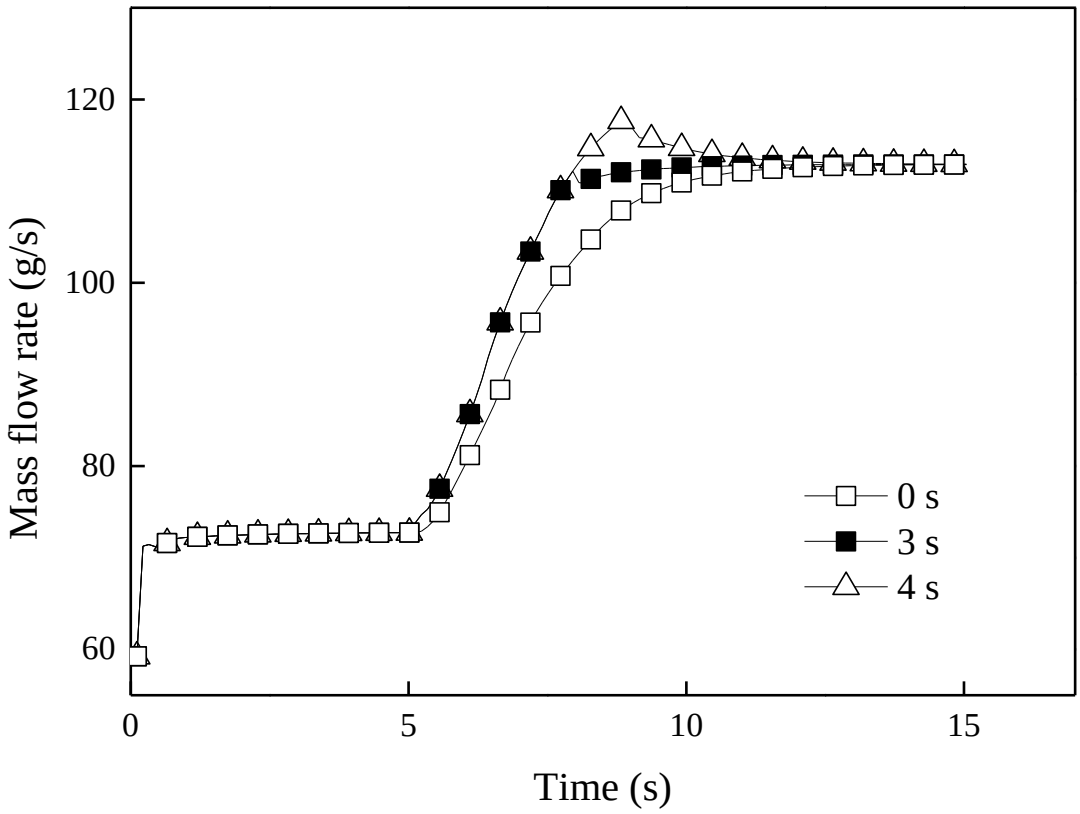

Fig. 14 Intake mass flow rate of the engine under different air injection durations

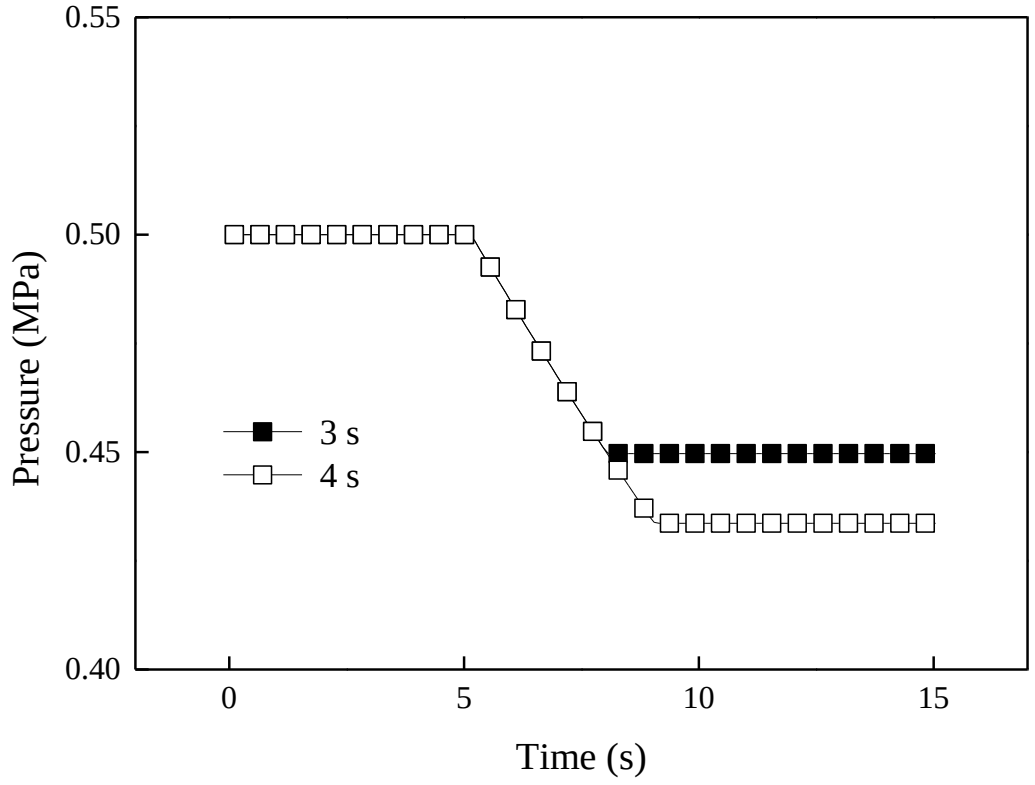

Fig. 15 Pressure variation of the air tank during the transient process

The pressure variation of the air tank during the transient process is shown in Fig. 15. It can be noted that the final pressure of the air tank is lower when a longer air injection duration is adopted. The final air tank pressure is 0.45 MPa when the injection duration is 3 s, while the tank pressure is decreased to 0.43 MPa if the air injection duration is extended 1 s longer. It can be predicted that the tank pressure will continue to decrease if the air injection duration is further extended. Hence, the positive effects of air injection boosting on the engine performance should be estimated against the consumption rate of the compressed air in practical application.

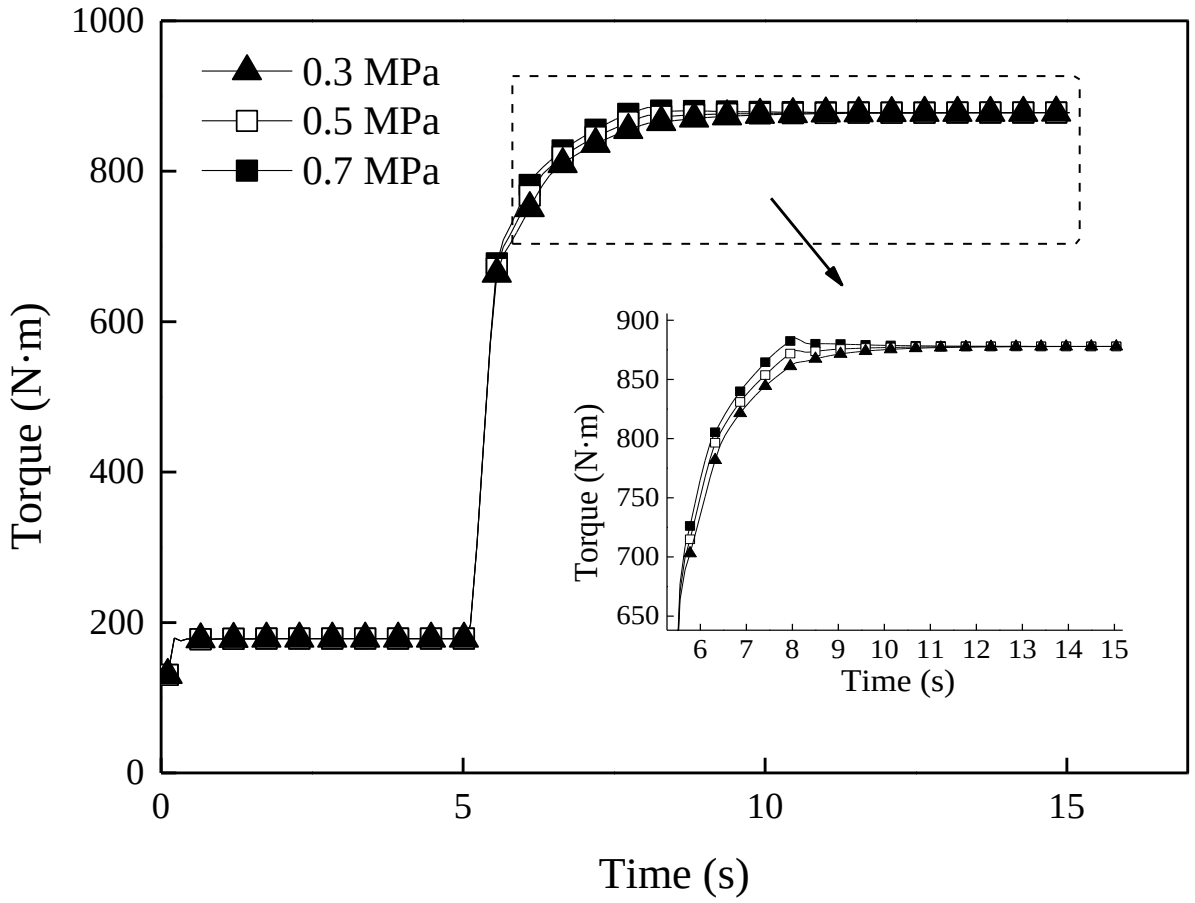

Fig. 16 Torque variations of the engine under different air tank pressures

The effects of air tank pressures on the engine performance during the transient process are illustrated in Fig. 16. Note that the air injection duration was maintained at 3 s under each tank pressure. As shown in Fig. 16, the air tank pressure has limited effect on the torque variation of the engine during the transient load

increase process since the torque difference between each tank pressure is less than 2%. The explanation is that the total intake flow mass of the engine has limited influence on the transient performance of the engine. As shown in Fig. 17, the maximum difference of intake mass flow rate is about 7%, however the effect of increased intake flow mass of the engine is weakened since the air injection duration is only 3 s. With the relatively short duration, the air injection with higher pressure is unable to leave sufficient influence on the intake flow of the engine. Considering the application of air injection boosting, lower air tank pressure is preferred since it is easier to reach during the regenerative braking process.

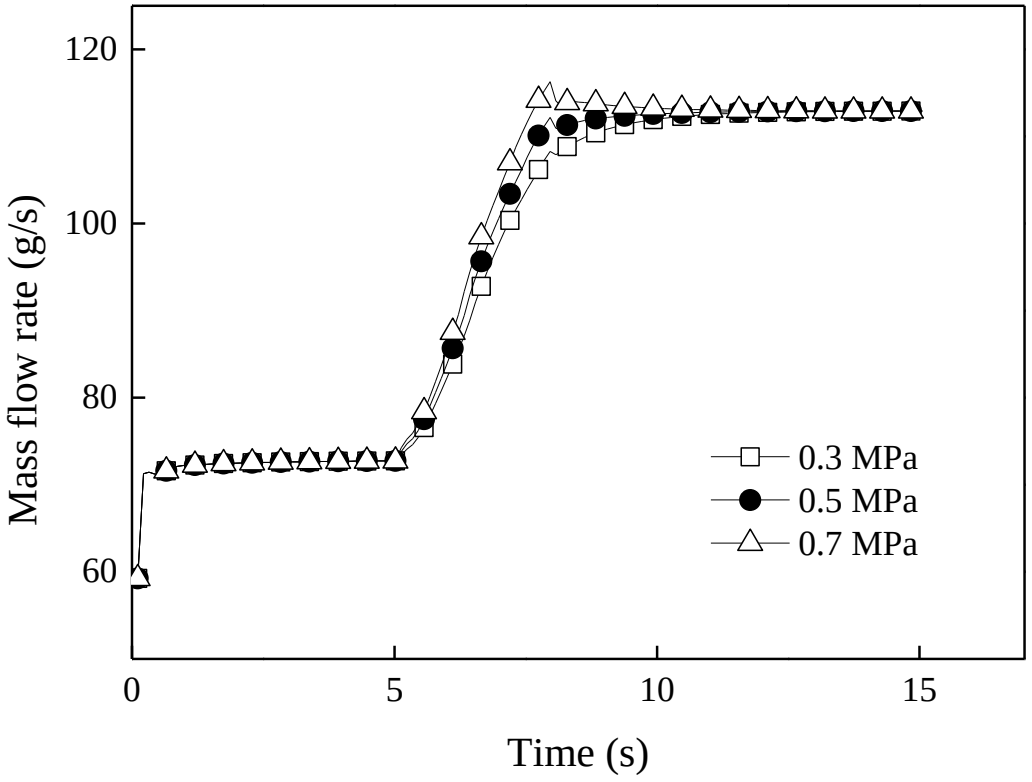

Fig. 17 Intake mass flow rate under different tank pressures

4 Conclusions

This study investigates the steady state and transient performance of a hybrid pneumatic combustion engine using direct injected air boosting system. The mathematic model of a hybrid pneumatic combustion engine is established. The hybrid pneumatic engine is simulated under both steady state and transient

conditions to investigate the effects of air injection boosting on its performance. The key findings can be summarised as follows:

- The power and BSFC of the engine can be improved when air injection boosting is used. Results indicate that the peak in-cylinder pressure is increased from 12.5 MPa to 14 MPa when the air injection boosting with the tank pressure of 0.5 MPa is adopted. At 1900 r/min and 100% load, the engine torque and power are raised from 1039 N·m, 206.9 kW to 1057 N·m, 210 kW. Results also show that the lowest BSFC is decreased from 200 kg/(kW·h) to 195 kg/(kW·h), showing a 2.5% improvement in the fuel economy of the engine when the AIB with the tank pressure of 0.5 MPa is adopted.
- The effects of air injection parameters on the engine performance are also analysed. Results show that the peak in-cylinder pressure is increased from 13 MPa to 14.7 MPa if the tank pressure is raised from 0.3 MPa to 0.7 MPa. The increase of tank pressure can also lead to a better performance of the engine in both power and fuel economy.
- Enlarging the diameter of the air injection hole can also lead to better engine performance. The simulation shows that an improvement of 5.8% can be achieved on the engine power. Moreover, the BSFC can be improved by 5.5% if the diameter of the air injection hole is increased from 3 mm to 7 mm.
- Analysis of the transient conditions shows that it takes about 5.5 s for the engine torque to be stabilised after an instant load increase if the air injection boosting is deactivated, indicating the existence of the turbo-lag. The responding time of the engine can be narrowed down to 3.5 s if an air injection boosting with 3 s duration is adopted. The extension of air injection duration can further reduce the effect of turbo-lag. In addition, the initial tank pressure has limited influence on the

transient performance of the engine due to the short injection duration.

In summary, this paper reports a simulation study of a hybrid pneumatic combustion engine using compressed air injection boosting to improve the steady state and transient performance of the system. The developed system can be potentially used for transport application by integrating with the internal combustion engine to recover the wasted kinetic energy during the braking process, and use the recovered energy to supercharge the engine to improve its overall efficiency and reduce the BSFC.

Acknowledgement

The authors would like to thank the support from the National Natural Science Foundation of China (Grant no. 51476143 and Grant no. 51806189) and from EPSRC through (EP/P001173/1) - Centre for Energy Systems Integration. The finical contribution from the NSFC-RS Joint Project under the grant number no. 5151101443 and IE/151256, China Postdoctoral Science Foundation under grant number 2018M640556 and from Zhejiang Province Postdoctoral Science Foundation under grant number ZJ20180099 are also highly acknowledged. The first author also would like to acknowledge the support from Funding Project for Young College Teachers of Shanghai under the grant No. ZZslg16006. The support from Cao Guang Biao High Tech Talent Fund, Zhejiang University is also highly acknowledged.

References

[1] Kim S-k, Fukuda D, Shimo D, Kataoka M, Nishida K. Simultaneous improvement of exhaust emissions and fuel consumption by optimization of combustion chamber shape of a diesel engine. International Journal of Engine Research. 2017;18:412-21.

[2] Singh R, Han T, Fatouraie M, Mansfield A, Wooldridge M, Boehman A. Influence of fuel injection strategies on efficiency and particulate emissions of gasoline and ethanol blends in a turbocharged multi-cylinder direct injection engine. International Journal of Engine Research. 2019:1468087419838393.

[3] Guan W, Pedrozo VB, Zhao H, Ban Z, Lin T. Miller cycle combined with exhaust gas recirculation and post–fuel

injection for emissions and exhaust gas temperature control of a heavy-duty diesel engine. International Journal of Engine Research. 2019:1468087419830019.

[4] Golzari R, Zhao H, Hall J, Bassett M, Williams J, Pearson R. Impact of intake port injection of water on boosted downsized gasoline direct injection engine combustion, efficiency and emissions. International Journal of Engine Research. 2019:1468087419832791.

[5] Rochussen J, McTaggart-Cowan G, Kirchen P. Parametric study of pilot-ignited direct-injection natural gas combustion in an optically accessible heavy-duty engine. International Journal of Engine Research. 2019:1468087419836877.

[6] Momenimovahed A, Liu F, Thomson KA, Smallwood GJ, Guo H. Effect of fuel composition on properties of particles emitted from a diesel–natural gas dual fuel engine. International Journal of Engine Research. 2019:1468087419846018.

[7] Wasbari F, Bakar RA, Gan LM, Tahir MM, Yusof AA. A review of compressed-air hybrid technology in vehicle system. Renewable and Sustainable Energy Reviews. 2017;67:935-53.

[8] Marvania D, Subudhi S. A comprehensive review on compressed air powered engine. Renewable and Sustainable Energy Reviews. 2017;70:1119-30.

[9] Shi Y, Li F, Cai M, Yu Q. Literature review: Present state and future trends of air-powered vehicles. Journal of Renewable and Sustainable Energy. 2016;8:025704.

[10] Li Y, Sciacovelli A, Peng X, Radcliffe J, Ding Y. Integrating compressed air energy storage with a diesel engine for electricity generation in isolated areas. Applied Energy. 2016;171:26-36.

[11] Basbous T, Younes R, Ilinca A, Perron J. Optimal management of compressed air energy storage in a hybrid wind-pneumatic-diesel system for remote area's power generation. Energy. 2015;84:267-78.

[12] Basbous T, Younes R, Ilinca A, Perron J. Pneumatic hybridization of a diesel engine using compressed air storage for wind-diesel energy generation. Energy. 2012;38:264-75.

[13] Basbous T, Younes R, Ilinca A, Perron J. A new hybrid pneumatic combustion engine to improve fuel consumption of wind–Diesel power system for non-interconnected areas. Applied Energy. 2012;96:459-76.

[14] Zhang X, Chen H, Xu Y, Li W, He F, Guo H, et al. Design and Performance Analysis of the Distributed Generation System Based on a Diesel Engine and Compressed Air Energy Storage. Energy Procedia. 2017;105:4492-8.

[15] Saad Y, Younes R, Abboudi S, Ilinca A. Hydro-pneumatic storage for wind-diesel electricity generation in remote sites. Applied Energy. 2018;231:1159-78.

[16] Schechter MM. Regenerative Compression Braking - A Low Cost Alternative to Electric Hybrids. SAE International; 2000-01-1025, 2000.

[17] Schechter MM. New Cycles for Automobile Engines. SAE International; 1999-01-0623, 1999.

[18] Dimitrova Z, Maréchal F. Gasoline hybrid pneumatic engine for efficient vehicle powertrain hybridization. Applied Energy. 2015;151:168-77.

[19] Dimitrova Z, Lourdais P, Marechal F. Performance and economic optimization of an organic rankine cycle for a gasoline hybrid pneumatic powertrain. Energy. 2015;86:574-88.

[20] Liu C-M, Wang Y-W, Sung C-K, Huang C-Y. The Feasibility Study of Regenerative Braking Applications in Air Hybrid Engine. Energy Procedia. 2017;105:4242-7.

[21] Dou WB, Li DF, Lu YJ, Yu XL, Roskilly AP. Evaluation of ideal double-tank hybrid pneumatic engine system under different compression cycle scenarios. Energy Procedia. 2017;142:1388-94.

[22] Bravo RRS, De Negri VJ, Oliveira AAM. Design and analysis of a parallel hydraulic – pneumatic regenerative braking system for heavy-duty hybrid vehicles. Applied Energy. 2018;225:60-77.

[23] Lee C-Y, Zhao H, Ma T. A simple and efficient mild air hybrid engine concept and its performance analysis. Proceedings of the Institution of Mechanical Engineers, Part D: Journal of Automobile Engineering. 2012;227:120-36.

[24] Lee C-Y, Zhao H, Ma T. Analysis of a novel mild air hybrid engine technology, RegenEBD, for buses and commercial vehicles. International Journal of Engine Research. 2012;13:274-86.

[25] Lee C-Y, Zhao H, Ma T. Pneumatic Regenerative Engine Braking Technology for Buses and Commercial Vehicles. SAE International Journal of Engines. 2011;4:2687-98.

[26] Wang L, Li DF, Xu HX, Fan ZP, Dou WB, Yu XL. Research on a pneumatic hybrid engine with regenerative braking and compressed-air-assisted cranking. Proceedings of the Institution of Mechanical Engineers, Part D: Journal of Automobile Engineering. 2016;230:406-22.

[27] Donitz C, Voser C, Vasile I, Onder C, Guzzella L. Validation of the Fuel Saving Potential of Downsized and Supercharged Hybrid Pneumatic Engines Using Vehicle Emulation Experiments. Journal OF Engineering for Gas Turbines and Power-Transaction of the ASME. 2011;133.

[28] Brejaud P, Higelin P, Charlet A, Colin G, Chamaillard Y. One dimensional modeling and experimental validation of single cylinder pneumatic combustion hybrid engine. SAE International Journal of Engines. 2011;4:2326-37.

[29] Trajkovic S, Tunestål P, Johansson B. A Simulation Study Quantifying the Effects of Drive Cycle Characteristics on the Performance of a Pneumatic Hybrid Bus. ASME 2010 Internal Combustion Engine Division Fall Technical Conference 2010: 605-18.

[30] Trajkovic S, Tunestal P, Johansson B. Vehicle driving cycle simulation of a pneumatic hybrid bus based on experimental engine measurements. SAE Technical Papers. 2010:2010-1.

[31] Donitz C, Vasile I, Onder CH, Guzzella L. Modelling and optimizing two- and four-stroke hybrid pneumatic engines.

Proceedings of the Institution of Mechanical Engineers, Part D: Journal of Automobile Engineering. 2009;223:255-80.

[32] Donitz C, Vasile I, Onder C, Guzzella L. Dynamic Programming for Hybrid Pneumatic Vehicles. Proceedings of the American Control Conference. 2009:3956-63.

[33] Andersson M, Johansson B, Hultqvist A. An Air Hybrid for High Power Absorption and Discharge. SAE Brasil Fuels & Lubricants Meeting. 2005.

[34] Higelin P, Vasile I, Charlet A, Chamaillard Y. Parametric optimization of a new hybrid pneumatic-combustion engine concept. International Journal of Engine Research. 2004;5:205-17.

[35] Higelin P, Charlet A, Chamaillard Y. Thermodynamic simulation of a hybrid pneumatic-combustion engine concept. International Journal of Thermodynamics. 2002;5:1-11.

[36] Fang Y, Lu Y, Yu X, Roskilly AP. Experimental study of a pneumatic engine with heat supply to improve the overall performance. Applied Thermal Engineering. 2018;134:78-85.

[37] Nie X-H, Yu X-L, Fang Y-D, Chen P-L. Experiment research on pneumatic diesel hybrid engine based on cooling water energy recovery. Neiranji Gongcheng/Chinese Internal Combustion Engine Engineering. 2010;31:58-62.

[38] Hu J-Q, Yu X-L, Nie X-H, Chen P-L. Feasibility of parallel air-powered and diesel hybrid engine. Zhejiang Daxue Xuebao (Gongxue Ban)/Journal of Zhejiang University (Engineering Science). 2009;43:1632-7.

[39] Zhai X, Yu X-L, Liu Z-M. Research on hybrid of compressed-air and fuel. Zhejiang Daxue Xuebao (Gongxue Ban)/Journal of Zhejiang University (Engineering Science). 2006;40:610-4.

[40] Wang L, Li D, Xu H, Fan Z, Dou W, Yu X. Research on a pneumatic hybrid engine with regenerative braking and compressed-air-assisted cranking. Proceedings of the Institution of Mechanical Engineers, Part D: Journal of Automobile Engineering. 2016;230:406-22.

[41] Heywood JB. Internal combustion engine fundamentals, 1988.

[42] Stanton DW. Systematic Development of Highly Efficient and Clean Engines to Meet Future Commercial Vehicle Greenhouse Gas Regulations. SAE International Journal of Engines. 2013; 6(3):1395-1480.